The International Journal of Advanced Manufacturing Technology (2018) 98:671–685
https://doi.org/10.1007/s00170-018-2298-x

ORIGINAL ARTICLE

Removal of critical regions by radius-varying trochoidal milling with constant cutting forces

Qing-Hui Wang[1] · Zhao-Yang Liao[1] · Yu-Xing Zheng[1] · Jing-Rong Li[1] · Xue-Feng Zhou[2]

Received: 28 January 2018 / Accepted: 5 June 2018 / Published online: 14 June 2018

Abstract
This work presents a novel milling strategy for complex pocket machining by integrating radius-varying trochoidal (RVTR) toolpath with contour parallel (CP) toolpath. Based on a quantitative analysis on the fluctuation of material removal rates (MRR), the proposed strategy is able to precisely identify critical regions from complex pocket geometries, and then by integrating flexible trochoidal radius with adaptive trochoidal step, the proposed approach is able to integrate the RVTR toolpath into CP toolpath under a consistent transition of material removal rate. Moreover, by applying RVTR toolpath, the cutting force can be maintained constantly when machining critical regions. Comparing with the trochoidal milling function available with current mainstream CAM software, experimental investigation has shown that the proposed RVTR-CP toolpath integration strategy offers a better machining condition with minimized fluctuation of cutting forces. Moreover, the total length of toolpath is decreased considerably and hence the machining efficiency is greatly improved.

Keywords Pocket milling · Critical milling regions · Trochoidal milling · Material removal rate · Cutting force control

1 Introduction

Constant cutting force is of great importance to the performance of milling applications, especially to high-speed milling (HSM) applications. Choy and Chan [1] reported that the cutting forces are sensitively affected by the cutter's engagement angle or the material removal rate (MRR) during milling process. For most toolpath generation strategies, the abrupt changes of MRR frequently occur. Taking the contour parallel (CP) toolpath as an example, it is the mostly used toolpath pattern for pocket milling, as illustrated in Fig. 1; the areas around sharp corners and the narrow slots formed by innermost contours always constitute the critical regions for machining. Ibaraki et al. [2] reported that the MRR for these critical regions is often subjected to abrupt changes and force strikes to the cutter are unavoidable, which may result in machining defects on the part, worse fatigue condition to the cutter, and more severely the direct breakage of the cutter. Moreover, such problem becomes more prominent for HSM or machining parts of hard materials. To tackle this problem, decreasing the depth of cut and using conservative constant feedrates have been the conventional measures to ensure the safety of machining. However, such conservative measures for NC machining cause considerable loss of machining efficiency. Therefore, maintaining relatively constant cutting forces during machining turns out to be a promising direction to further improve machining efficiency.

Over the past decade, a number of research efforts have been made to address the problem of cutting force fluctuation by maintaining the MRR as constant as possible. These approaches can be classified into either using adaptive feedrates or keeping a relative constant material engagement angle using optimized toolpath. Tarng and Chen [3] proposed a fuzzy control method to optimize feedrate at real time. They concluded that the optimized feedrate is able to satisfy the requirements of constant MRR. Erdim et al. [4] presented a feedrate optimization strategy for surface milling to achieve constant MRR and cutting forces. Uddin et al. [5] proposed a new offset algorithm to generate CP toolpath, which regulates the cutting engagement angle at a desired value in the 2D milling. Karunakaran et al. [6] developed a simulation system based on an instantaneous cutting force model, in which the

✉ Jing-Rong Li
lijr@scut.edu.cn

[1] School of Mechanical and Automotive Engineering, South China University of Technology, Guangzhou 510641, China

[2] Guangdong Institute of Intelligent Manufacturing, Guangzhou 510070, China

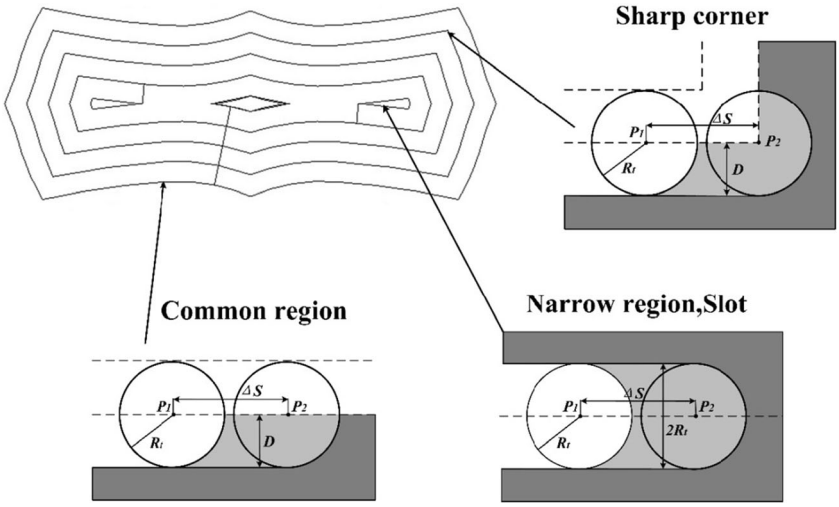

Fig. 1 Illustration of critical regions along CP toolpaths

feedrate can be adjusted so as to maintain a relatively stable cutting force. However, since the cutting force and MRR always increase rapidly at critical regions, solely using adaptive feedrate is difficult to completely avoid the instantaneous force increase at sharp corners.

On the other hand, approaches based on toolpath's geometric optimization are able to address the problem with more resources. Choy and Chan [7] attempt to minimize the shock of cutting forces by inserting additional bow-type looping toolpaths at corner areas. And it is so promising that the approach has been realized by some latest commercial CAM systems already. Kim et al. [8] reported a method to insert additional looping segments into CP toolpaths and concluded that the optimized toolpath can effectively control the variation of MRR. Held and Spielberger [9] developed an approach using smooth spiral toolpaths instead of conventional CP toolpaths for pocket milling, which have demonstrated improved smoothness of transition between two neighboring contours of toolpath; however, the abrupt change of MRR still cannot be eliminated completely.

In recent years, trochoidal (TR) toolpaths have been proposed to address the problem of cutting force fluctuation. According to Rauch et al. [10], there are two types of geometrical models for TR toolpaths: the circular TR model and the standard TR model. The former uses straight line segments tangent to adjacent circles, which come with C^1 continuity, whereas the latter generates a more complex path and normally with C^2 continuity, and hence, it is favorable to the kinematic behavior of machine tool. Ibaraki et al. [2] demonstrated that the main advantage of TR milling lies in that it can effectively control the variation of engagement angle and radial depth of cut (RDC). With this control, critical cutting conditions, such as abrupt change of MRR and full angle engagement of cutting, can be avoided. Therefore, it offers a more stable cutting condition for machining critical regions with higher feedrate. Elber et al. [11] presented an algorithm of generating trochoid cycles based on medial axis algorithm and employed it to groove critical regions. Rauch et al. [10] claimed that the maximal RDC for TR toolpaths can be calculated by a so-called process constraint model, whose constraints include the values of tool radius, the circular movement radius, and the center displacement distance. More recently, based on regional segmentation according to the radius change of locally inscribed circles along the media axis of a cavity, Ferreira and Ochoa [12] proposed a new TR toolpath strategy for pocket milling process with different cutter diameters. Moreover, in their approach, the TR toolpath was optimized through a pixel-based simulation to reduce the problem of idle cutting, which however breaks the C^2 continuity of the toolpath. Wu et al. [13, 14] inserted a sequence of circular cycle toolpaths at corners for milling sharp corners, where the cutting load always changes drastically with most conventional toolpath. Deng et al. [15] developed a formula to predict cutting force for trochoidal milling and then proposed a toolpath optimization model to achieve shortest machining time under expected cutting forces. The method of RDC control along TR trajectory has also been introduced into the process of plunge milling. With the precise control of RDC for each cutter location, considerable improvements have been demonstrated for both cutting efficiency and cutter's life in plunge milling [16].

Although existing research efforts tried to address the problems of cutting force fluctuations at critical regions, there still lacks reasonable method to precisely recognize the so-called critical regions from the complex pocket region of machining. More importantly, the length of TR toolpaths is generally much longer than that of conventional CP toolpaths, and certainly, it is inefficient to apply TR toolpath at the rest of so-called common regions, where MRR changes little. Therefore, it is necessary to generate optimal toolpaths with constant MRR and with high efficiency as well. In authors' previous work [17], a radius-varying TR (RVTR) toolpath model was

proposed. With the varying evolution radius, most critical regions can be machined by a single strip of the RVTR toolpath. Furthermore, a method of adaptive trochoidal step control was developed for the RVTR toolpath, so as to maintain a constant RDC among each TR milling cycle with different radii. As a continuous effort, this work focuses on the approach to precisely integrating the RVTR trajectory with conventional CP toolpath. Based on a quantitative analysis of MRR fluctuation, the proposed toolpath integration strategy is able to precisely identify critical regions from complex pocket geometries and then to mill the entire pocket in one go using RVTR trajectories for critical regions and CP toolpaths for the rest. Control algorithms are developed to ensure that the connection between RVTR trajectories with neighboring CP toolpaths is geometrically continuous and under very consistent MRR transition as well. Therefore, an almost constant cutting force can be maintained for the entire pocket machining, and hence considerable improvements on machining efficiency can be achieved.

The remainder of the paper is organized as follows: Section 2 presents a pixel-based MRR simulation method for identification of critical regions. The RVTR-CP integration strategy and its control algorithms are presented in Section 3. Section 4 explains the implementation of the proposed approach, followed by a performance comparison with the commercial available toolpath strategy by SIEMENS NX®. Section 5 concludes the work.

2 Identification of critical milling regions

Ibaraki et al. [2] proposed the concept of critical milling region and used the width of the narrow slot to distinguish the critical regions. The unique characteristic of these critical milling regions is that the cutting forces fluctuate inevitably during its milling process. As illustrated in Fig. 1, for most pocket milling cases along conventional CP toolpaths, the sharp corners, narrow milling regions, and slots are generally considered as critical milling regions, due to the fact that the cutting forces in these regions are with considerable fluctuations. However, there is no report yet on how to automatically identify these critical regions from arbitrary pocket machining cases. In this section, an automated algorithm is developed to identify critical regions according to the analysis of MRR variations. Its procedures are as follows:

Procedure 1: pixel-based MRR simulation. For a given pocket machining case, its MRR variation along toolpath is simulated using a pixel-based algorithm under a predetermined controllable precision.

Procedure 2: segmentation of critical toolpaths. Based on the analysis of MRR profile along the toolpath, the entire toolpath is further segmented into a set of trajectory segments with two types, i.e., the critical toolpath and common CP toolpath. Basically, the trajectories raising MRR variation more than a predetermined threshold are considered as critical toolpath, and the rest with relatively stable MRR are considered as common toolpath.

Procedure 3: creation of critical regions. This procedure is to organize the neighboring but tessellated critical toolpath segments into several regional connected critical regions with enclosed profiles, which will be identified for further TR milling.

2.1 Pixel-based MRR simulation

MRR here is calculated as the volume of material removed per minute. As illustrated in Fig. 1, for the simplest toolpath geometries when milling common regions, i.e. a linear toolpath trajectory or a curved toolpath trajectory with no curvature change, the *MRR* is at a stable level as follows:

$$MRR_{exp} = \frac{MRV}{t} = \Delta S \cdot D \cdot Adc / t \tag{1}$$

where *MRR_exp* represents the expected value of MRR and *MRV* represents the volume of material removed during the time span t; ΔS is the distance of the toolpath trajectory, D is the interval of CP toolpath, Adc represents the axial depth of cut, and t can be computed by:

$$t = \Delta S / f \tag{2}$$

where f represents the feedrate of the motion.

Therefore, the expected MRR for most common regions machining can be simply expressed as:

$$MRR_{exp} = D \cdot f \cdot Adc \tag{3}$$

However, as illustrated in Fig. 1, the toolpath trajectory tends to be degenerated at those regions such as sharp corners and most-inner loops. The MRR around these critical regions is always with big fluctuation; hence, it is difficult to analytically compute the MRR using Eq. (3) for any arbitrary toolpath. To address the MRR computation problem for arbitrary machining cases, a pixel-based MRR simulation method proposed by Kim et al. [8] is adopted in this work. As an initial process, the machining region is discretized first and represented as pixel squares with a controlled resolution. When cutter moves along a toolpath, its cutting area can be computed by the number of the pixel squares swept. As illustrated in Fig. 2, when a cutter moves from location P_{i-1} to location P_i, the corresponding MRR can then be approximately computed according to the pixel-based simulation.

Figure 3 shows an example of simulated MRR along the CP toolpaths in Fig. 1. By observing the simulation graph, the MRR appears to be stable with the majority toolpath

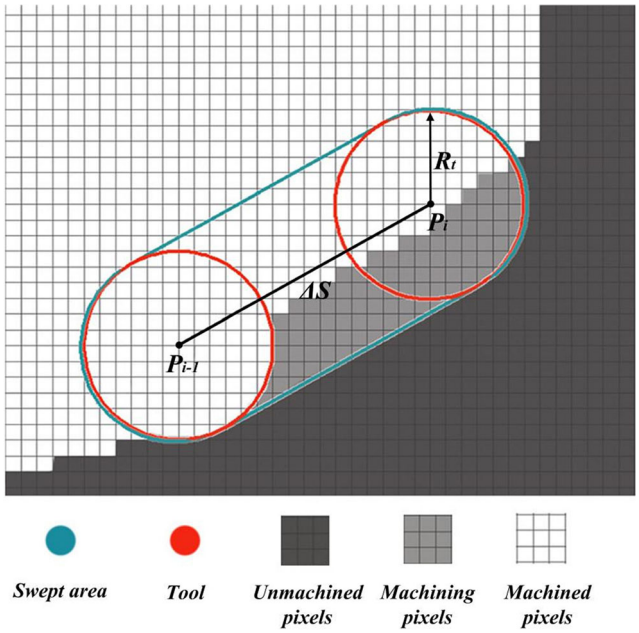

Fig. 2 Pixel-based MRR simulation

trajectories for common region machining, with its value around MRR_{exp}. However, when the cutter moves into critical regions, such as narrow slots or sharp corners, abrupt MRR changes can be observed at a regular frequency, with its instantaneous value up to triple of the stable value. The example demonstrated that the pixel-based MRR simulation can be used to predicate the MRR fluctuations for a given toolpath, which helps to locate the critical regions in advance, so as to replace the CP toolpath with regional TR toolpath for better machining performance.

2.2 Segmentation of critical cutter locations

Taking the MRR graph in Fig. 3 as an example, in order to find all the critical regions, firstly, it needs to locate the exact cutter locations that raise a MRR change obviously exceeding a stable level, which requires a reasonable threshold value. However, as observed from Fig. 3, there exists obvious MRR fluctuations around the cutter locations when a cutter is under transition between common and critical regions. Experimental study shows that the MRR fluctuation graphs during the stage of cutting transition are with big variation for different machining cases, it does not always converge to the expected stable level of MRR, the MRR_{exp} by Eq. (3). Therefore, instead of simply taking MRR_{exp} as the fixed threshold value, based on Otsu algorithm, an adaptive threshold method is developed in this work to determine the threshold. The Otsu algorithm first proposed by Ohtsu [18] is known as one of the robust methods in computing the optimal threshold that maximizes the separability of two classes of values. Being a histogram-based and automatic approach, it has been extensively used in image segmentation to produce an objective result unbiased by spatial information. This threshold determination method for the critical region segmentation is described as follows.

For a given toolpath, which is represented by a list of discretized cutter locations, and denoted by $CL_{list} = \{cl_1, cl_2, \ldots, cl_N\}$, each element $cl_i \in CL_{list}$ has a computed MRR value

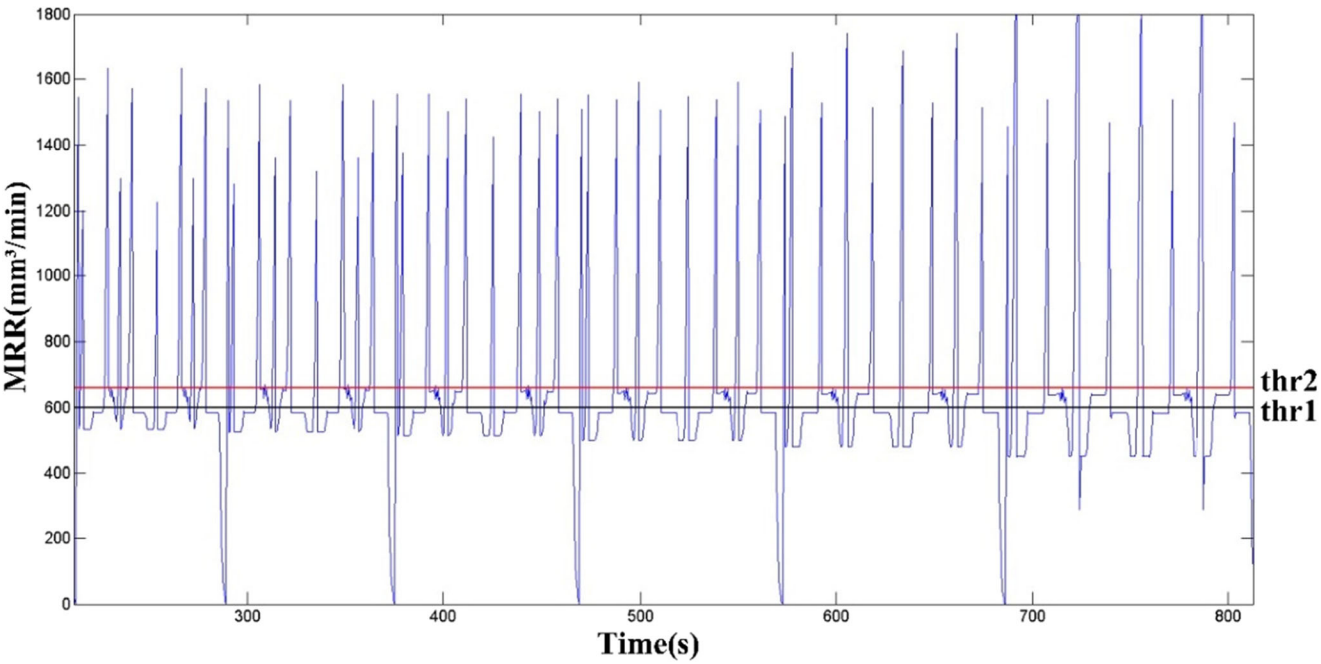

Fig. 3 Simulated MRR distribution along CP toolpaths

$mrr(i) \in [0, MRR_{max}]$. Assuming a threshold value, MRR_{thr}, is used to dichotomize the cutter locations in CL_{list} into two classes, i.e., the class of target region, or the critical milling region, $CL_{cri}(MRR_{thr}) = \{\cup cl_i, MRR_{thr} \le mrr(i) \le MRR_{max}\}$, and the class of background region, or the common machining region, $CL_{com}(MRR_{thr}) = \{\cup cl_i, o \le mrr(i) \le MRR_{thr}\}$. The probabilities of class occurrence of $CL_{cri}(MRR_{thr})$ and $CL_{com}(MRR_{thr})$ are computed as the ratio of the accumulated length of the toolpath segments in the respective class to the total length of entire toolpath, represented by $p_{cri}(MRR_{thr})$ and $p_{com}(MRR_{thr})$, respectively.

For a discretized toolpath containing m cutter locations, the mean level of MRR of the toolpath is given by:

$$\mu = \frac{\sum_{i=1}^{m-1} length(cl_i, cl_{i+1}) \cdot mrr(i)}{\sum_{i=1}^{m-1} length(cl_i, cl_{i+1})} \tag{4}$$

Based on Eq. (4), the mean level of MRR for $CL_{cri}(MRR_{thr})$ and $CL_{com}(MRR_{thr})$ can be computed, respectively, and denoted using $\mu_{cri}(MRR_{thr})$ and $\mu_{com}(MRR_{thr})$. And assuming the mean MRR for the entire region of machining is μ_{reg}, the between-class variance for the choice of MRR_{thr} is then formulated as:

$$\sigma_B^2(MRR_{thr}) = p_{cri}(MRR_{thr})\left[\mu_{cri}(MRR_{thr}) - \mu_{reg}\right]^2 + p_{com}(MRR_{thr})\left[\mu_{com}(MRR_{thr}) - \mu_{reg}\right]^2 \tag{5}$$

By observing the Eq. (5), $\sigma_B^2(MRR_{thr})$ is an objective function with decision variable $MRR_{thr} \in [0, MRR_{max}]$. Therefore, the problem of threshold determination turns out to be an optimization problem instead to search for the optimal value for MRR_{thr} to maximize the objective function. Figure 4 shows an example of MRR distribution for CP toolpath based machining. It uses a flat end cutter of *6* mm in diameter, taking CP toolpath interval $D = 2$ *mm*, the axial depth of cut $Adc = 3$ mm, and the feedrate $f = 100$ mm/min. The simulated MRR values for machining the entire region are distributed within [0, 1800], and the optimal global threshold is determined as $MRR_{thr} = 600$ mm^3/min, which is identical to the expected MRR level for common regional machining, i.e., the computed MRR_{exp} by Eq. (3). However, if simply taking the optimal global threshold to segment critical machining regions, it will include a considerable portion of unnecessary cutter locations into the segmentation result as exampled in Fig. 4b, since most of these cutter locations do not arise any abrupt change of MRR, but having their MRR values slightly fluctuated around MRR_{exp}. Therefore, we have to find a more reasonable local threshold within the range of (MRR_{exp}, MRR_{max}] using above algorithm. Figure 4c shows the segmentation results of critical cutter locations, which is based on the local threshold $MRR_{thr} = 713$ mm^3/min. Obviously, using the local threshold offers more reasonable segmentation results, since it helps to prevent excessive TR toolpath from machining.

2.3 Contour fitting of critical region

The segmentation method discussed above provides a quantitative way to locate the critical cutter locations from the common CP toolpath. However, the segmented critical toolpath is tessellated, and it is difficult to define TR milling regions simply based on these tessellated segments. It is desirable to organize these critical toolpath segments into a number of enclosed regions for further regional TR milling.

In this work, a contour fitting method based on so-called α-shape algorithm is developed to obtain the minimal enclosed profile for a critical region definition. The α-shape algorithm was proposed by Edelsbrunner et al. [19] and has been generally used to address the boundary detection problem for a set of finite points, with a parameter α to control the boundary detection effect adaptive to the density of the point set. The α-shape can be derived from the α-hull, which is a generalization of convex hull, and when $1/\alpha \to \infty$, α-shape turns to a convex hull. As shown in Fig. 5, the α-shape is defined by a lot of discs with radius $1/\alpha$. In order to get a satisfied detection effect, the key factor is to appropriately determine the α-parameter. In theory, the smaller $1/\alpha$ is, the more sensitive the α-shape algorithm to the distribution density of the point set. Figure 6 shows the resulted critical regions by using the α-shape algorithm by taking $1/\alpha = 2D$, where D is the interval between two neighboring parallel contours.

3 Integration between RVTR and CP toolpaths

3.1 The model of RVTR toolpath

In recent years, several types of trochoidal-like toolpaths have been proposed to address the issue of cutting force fluctuation when milling critical regions. Generally, these trochoidal-like toolpaths are implemented using three types of model. The first type is based on *circular model*, which is represented as a sequence of consecutive circular curves, and linked with a linear segment tangent to adjacent circles with C^1 continuity. The second type, which was mentioned in reference [20], is a classic TR model that uses a constant radius for trochoidal evolution. It is able to generate TR toolpath with C^2 continuity. The third type is the so-called RVTR toolpath, which was proposed in authors' previous work [17]. Comparing with the classic TR model, the RVTR toolpath comes with two main advantages. One is that the radius for TR evolution can vary, which makes the toolpath flexible enough to fit into complex machining regions simply along a guiding path. Secondly, the step for each TR evolution can adapt to the varying radius, so

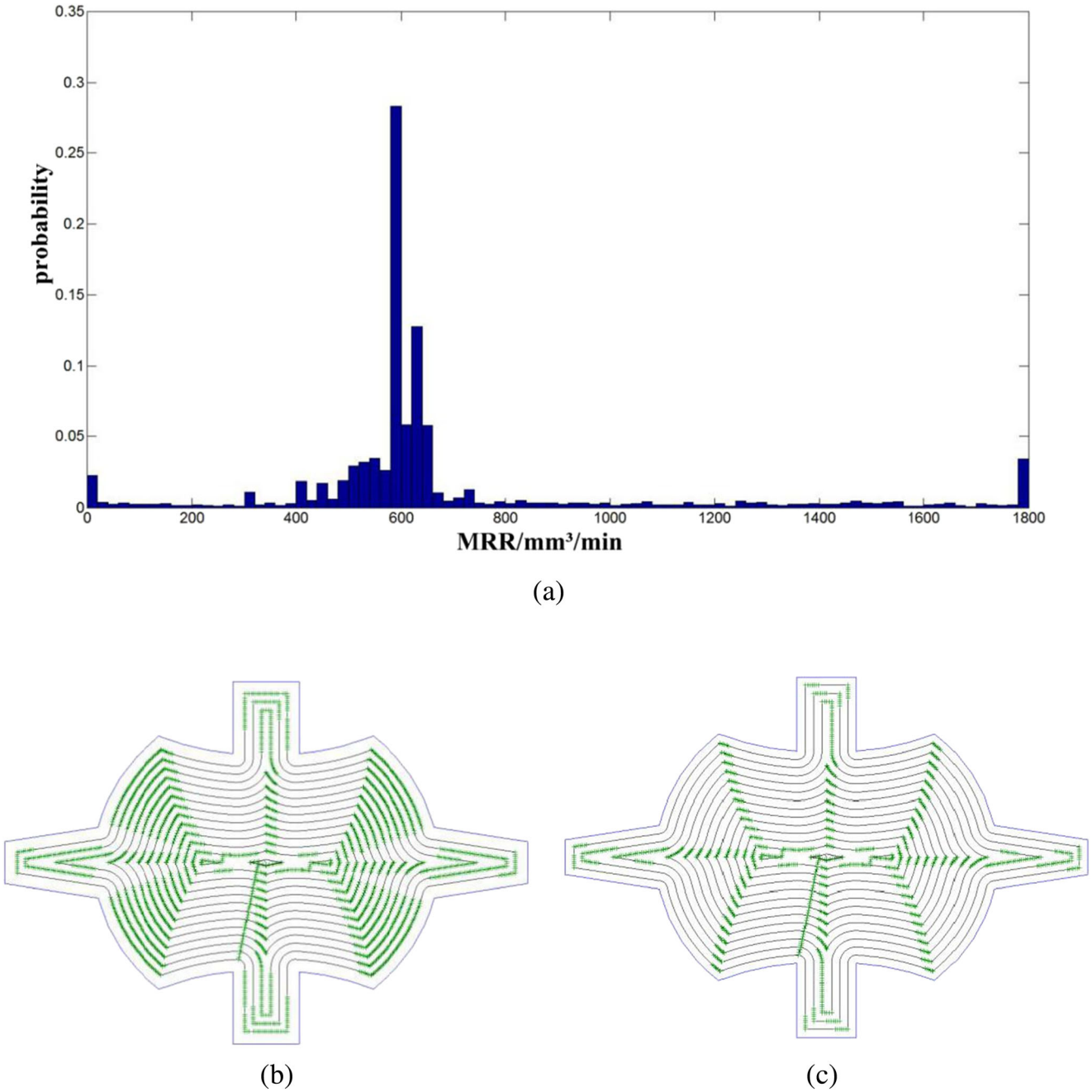

Fig. 4 Identification of critical cutter locations based on MRR threshold. **a** Histogram analysis of MRR distributions. **b** Segmentation results by global threshold $MRR_{thr} = 600$ mm^3/mi. **c** Segmentation results by local threshold $MRR_{thr} = 713$ mm^3/min

as to maintain a constant maximal RDC no matter the change of evolution radius. Because of these two advantages, the RVTR toolpath is better in machining critical regions.

In order to fill the RVTR toolpath into a complex machining region, the so-called medial axis algorithm is used as the first step to generate a guiding path for a given region, and then the TR toolpath moves their instantaneous centers along the guiding path. In this work, the medial axis computation is completed using Voronoi diagram-enabled algorithm [21].

Once the a guiding path of a machining region is available, the next step is to determine the TR radius together with its adaptive step length for each cycle of TR evolution, so as to make the TR toolpath can well fit into the region, while keeping constant RDC for each cycle of machining. As illustrated in Fig. 7, the toolpath is modelled as a TR cycle with its instantaneous center moving linearly from O_1 to O_2. O_1 and O_2 are located on the guiding path with a distance S_{step}, the current step for TR evolution. The instantaneous center is denoted as

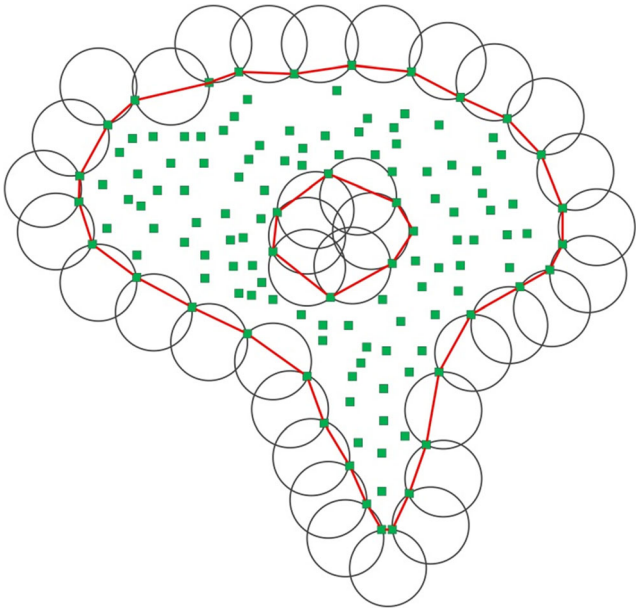

Fig. 5 An example of boundary detection for a set of points using α-shape algorithm

$O(\theta)(X_O, Y_O)$, which can be parameterized by the revolution angle, $\theta \in [0, 2\pi]$.

$$\begin{cases} X_O(\theta) = O_{1.x} + \overrightarrow{O_1O_2} \cdot \vec{X} \dfrac{\theta}{2\pi} \\ Y_O(\theta) = O_{1.y} + \overrightarrow{O_1O_2} \cdot \vec{Y} \dfrac{\theta}{2\pi} \end{cases} \tag{6}$$

During the TR evolution, since the TR radius varies following the change of θ, it is hereby denoted as $R_{TR}(\theta)$. The cutter location $C(\theta)(X_C, Y_C)$ is on the TR curve and having the distance of $R_{TR}(\theta)$ to the instantaneous center $O(\theta)$.

$$\begin{cases} X_C(\theta) = O(\theta)_{.x} + R_{TR}(\theta) Sin\theta \\ Y_C(\theta) = O(\theta)_{.y} + R_{TR}(\theta) Cos\theta \end{cases} \tag{7}$$

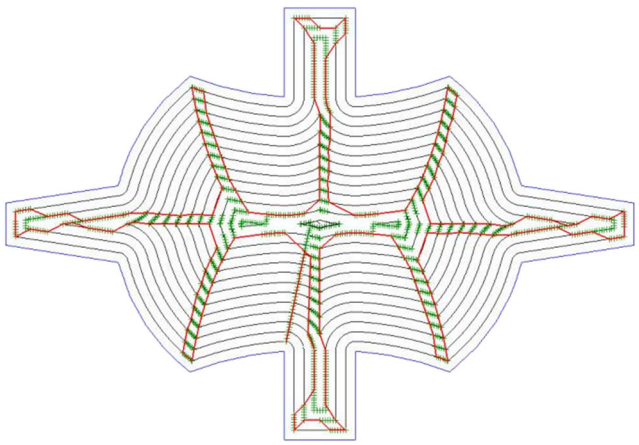

Fig. 6 An example contour fitting for critical regions using α-shape algorithm

The milled profile left on the part by the period of TR toolpath is the cutter contact point and being represented by $P(\theta)(X_P, Y_P)$ here as,

$$\begin{cases} X_P(\theta) = O(\theta)_{.x} + (R_{TR}(\theta) + R_{tool}) Sin\theta \\ Y_P(\theta) = O(\theta)_{.y} + (R_{TR}(\theta) + R_{tool}) Cos\theta \end{cases} \tag{8}$$

Using R_1 and R_2 to represent the radii of the inscribed circles centered at O_1 and O_2, respectively, the instantaneous TR radius $R_{TR}(\theta)$ during the cycle of TR revolution is considered as the linear interpolation between R_1 and R_2 and can be parameterized by the revolution angle $\theta \in [0, 2\pi]$.

$$R_{TR}(\theta) = (R_1 - R_{tool}) \left(1 - \frac{\theta}{2\pi}\right) + (R_2 - R_{tool}) \frac{\theta}{2\pi} \tag{9}$$

Figure 8a gives a typical example of computed medial axis with a complex machining region. Along the medial axis curve, TR toolpath is generated with varying radius exactly fitting into the region (Fig. 8b).

3.2 Adaptive TR steps for constant RDC

As reported by Kloypayan and Lee [22], the cutting force is sensitive to the variation of MRR during a milling process. Under the TR milling mode, the cutter engagement angle is much more stable while machining; thus, the RDC becomes the dominate factor to affect the variation of MRR and the actual cutter forces. Therefore, it is necessary to keep the RDC being constant for all TR milling cycles. The RDC of TR toolpath is determined by both values of the TR radius and the step. If using a constant TR step, the varied TR radius will result in varied RDC for each milling cycle. In order to maintain a constant RDC, the TR step must to be adaptive to the varied TR radius.

Rauch et al. [10] presented a method to calculate maximal RDC based on circular TR model. However, the RVTR model is different from the circular model, since it is difficult to compute the value of RDC by analytic geometry. In this work, a numerical method reported in reference [17] was used to compute adaptive TR step, which can make the maximal RDC of each milling cycle converged at an expected value.

More than to maintain constant MRR for TR milling, the RDC control is also the key measure to guarantee a consistent MRR transition between TR and CP toolpaths for the proposed RVTR-CP integration. As illustrated in Section 2.1, after the removal of critical regions, machining along CP toolpath has a constant MRR, which is the MRR_{exp} as formulated by Eq. (3). To guarantee a consistent MRR transition between TR and CP toolpaths, the RDC value for TR toolpath can be determined as,

$$Rdc_{\exp} = \frac{MRR_{\exp}}{Adc \cdot f} \tag{10}$$

where Rdc_{exp} is the RDC expected; it is equivalent to the toolpath interval D of CP toolpath.

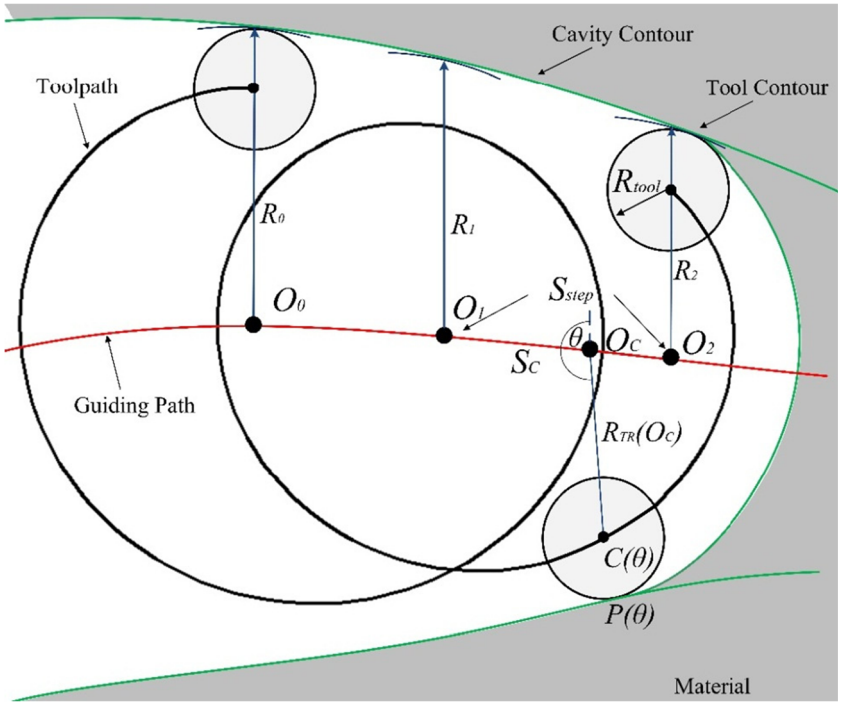

Fig. 7 The generation model of RVTR toolpath

3.3 Connecting RVTR toolpath with CP toolpath

As illustrated above, the TR toolpath generated along medial axis curves can perfectly fit into a complex pocket region. These curves have been extensively used as the guiding path for TR milling of pocket regions. However, in this work, other than the fitting of RVTR toolpath into critical regions, the smooth connection between the generated RVTR toolpath and its neighboring CP toolpaths is another important concern. Furthermore, in most CP milling applications, the recognized critical regions can be generally classified into two typical regions, i.e., *narrow critical regions* and corner *critical regions*. The RVTR-CP integration methods at the two types of regions are also different. They are discussed separately as follows:

- *RVTR-CP integration at narrow critical region*

  A *narrow critical region* is usually identified at the narrow slot areas of a pocket or at the area of inmost contours of CP toolpath. As exampled in Fig. 9a, for the segmented narrow critical region, all medial axis curves of the current contour are generated first. In order to guarantee the critical region machining completed by a single strip of TR milling, only the main branch of the medial axis curve is selected, and those outermost branches are excluded from being guiding path. Moreover, not the overall main branch of medial axis curve is used. A further trim operation truncates a small portion of the curve by a neighboring sub-contour and using the left portion of the curve only as the guiding path for TR toolpath generation. As illustrated in Fig. 10c, d, after the truncation, the generated TR toolpaths can then have a very smooth connection with CP toolpaths.

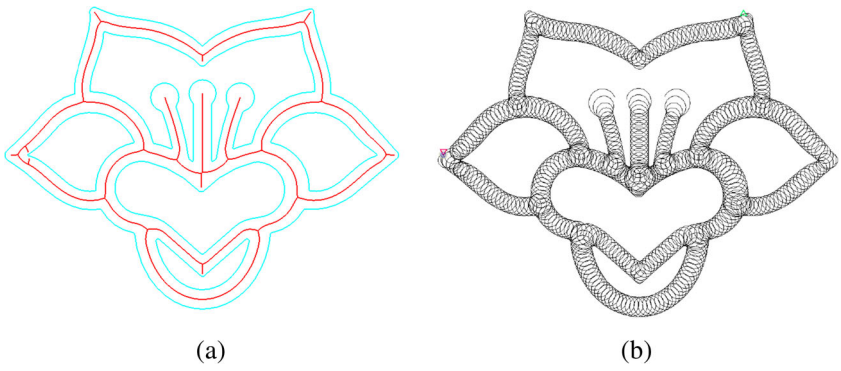

Fig. 8 Example of fitting RVTR toolpath into complex machining region. **a** Computation of medial axis. **b** RVTR toolpath generation along medial axis

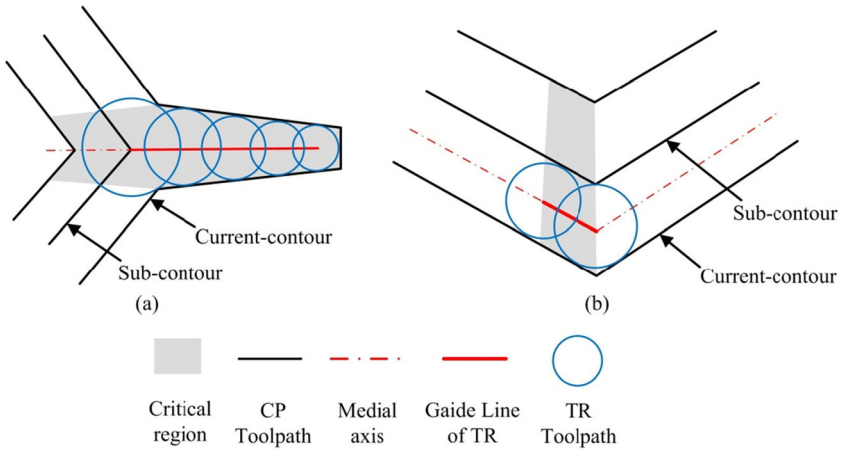

Fig. 9 Generation of guide path from medial axis. **a** Guiding path for narrow critical region. **b** Guiding path for corner critical region

- *RVTR-CP integration at sharp corner region*

  A sharp corner region usually occurs when the toolpath changes direction abruptly. The generation of guiding path for a sharp corner region is different from that for narrow critical regions. As illustrated in Fig. 9b, for a sharp corner region, all medial axis curves between the current contour and its sub-contour are generated first. Similarly, only the medial axis curve inside the critical region (the gray area in Fig. 9b) is selected as the guiding path, which ensures the generated TR toolpath well connected with CP toolpath under tangency continuity. Moreover, when

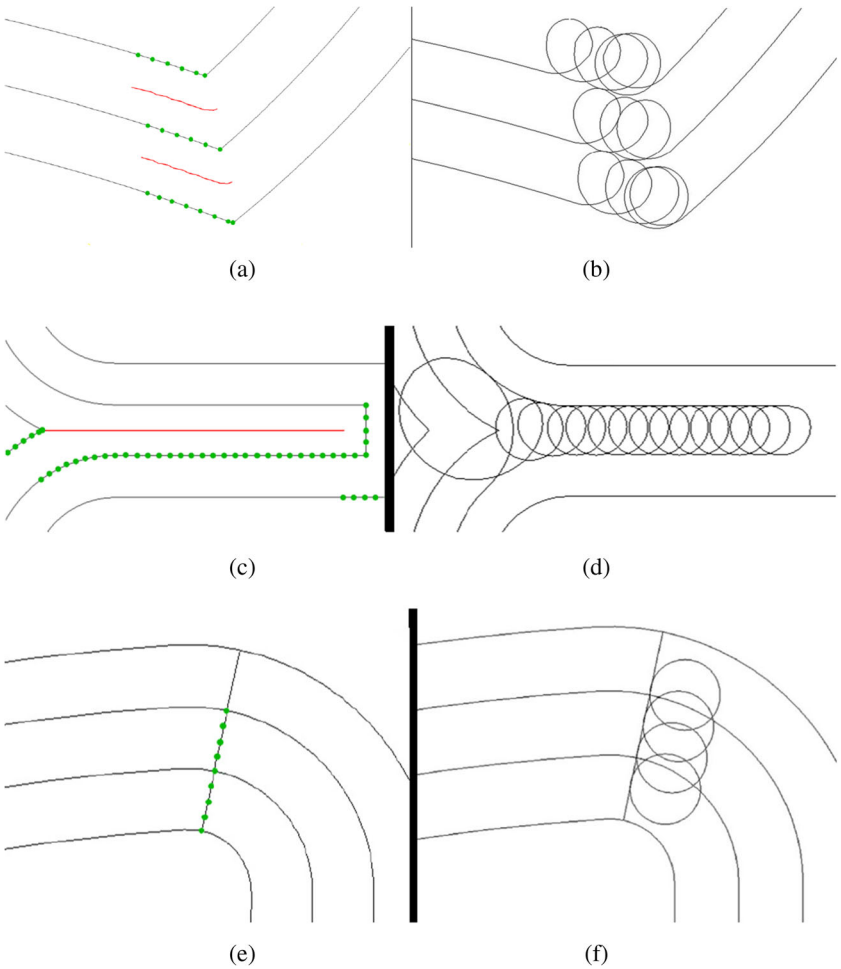

Fig. 10 Integrating RVTR toolpath with CP toolpath. **a** Critical CLs and guiding oath at corner region. **b** TR toolpath integration at corner region. **c** Critical CLs and guiding path at narrow region. **d** TR toolpath integration at narrow region. **e** Critical CLs for moving across contour. **f** TR toolpath integration for moving across contour

a cutter moves between two parallel contours, the MRR may suffer abrupt changes and critical cutter locations will be identified around there as illustrated in Fig. 10e. This problem has been a typical issue with conventional CP milling. In this work, to solve this problem, a small portion of TR toolpath is added to optimize the direct linear connection between parallel contours (Fig. 10f).

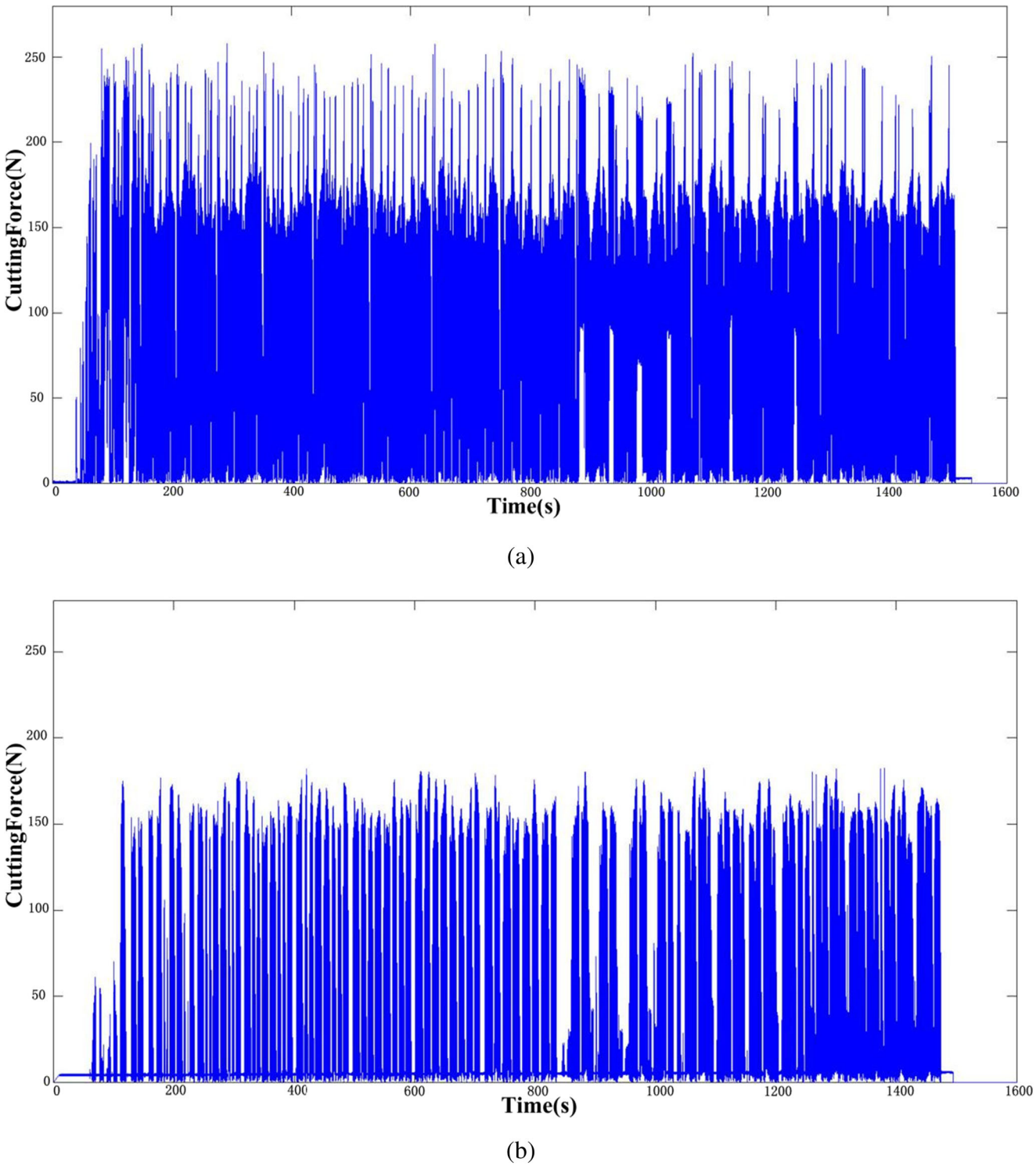

Fig. 11 Cutting force measurement along CP toolpath. **a** Critical region existed. **b** Critical region removed

With the above algorithm, RVTR toolpath can be generated to fill in each critical regions with C^1 continuity to the neighboring CP toolpaths, as illustrated in Fig. 10b, d, f. Moreover, by using the algorithm of adaptive TR steps (Section 3.2), the cutter's movement between the TR and CP toolpath is under very consistent MRR transition as well, which theoretically offers an ideal condition of constant cutting force for machining the entire pocket.

4 Performance evaluations for RVTR-CP strategy

In this section, experimental comparisons are carried out to evaluate the performances of the proposed RVTR-CP toolpath strategy. As shown by Fig. 6, the pocket part used is with complex geometric boundary, which generates a number of narrow regions and sharp corners when using conventional CP toolpath and therefore results in many critical regions during machining. Using the pixel-based critical region recognition algorithm proposed in Section 2, these critical regions with CP toolpath are identified as shown in Fig. 6. Certainly, this part is suitable to apply RVTR-CP integrated toolpath because of the frequent occurrence of critical regions.

The first test is to examine the accuracy of critical region recognition of the proposed algorithm. And then, second experiment is carried out to further evaluate the performance of the RVTR-CP toolpath for its machining efficiency and level of cutting force fluctuation. More specifically, the comparison is made between proposed approaches with the TR toolpath generated by commercial CAM software SIEMENS NX®.

4.1 Accuracy of identifying critical regions

One identical experiment is carried out here to machine the pocket in Fig. 6 under two different conditions respectively: one is to remove critical regions with the proposed identification method and another is without identification. Moreover, while machining, the cutting force variation along toolpaths is recorded. The part material is 6061 aluminum alloy, and the machining uses a flat end cutter with a diameter of 6 mm. The force measuring system uses a quartz three-component dynamometer, Kistler 9257A, which is able to sample the cutting forces at a frequency of 600 Hz.

In the first run of machining, the pocket is machined using CP toolpath with all critical region existed. Figure 11a shows the diagram of measured cutting forces, from which many abrupt cutting force fluctuations can be observed with the range from around 150 N to the maximum of around 250 N.

In the second run of machining, the critical regions are removed from the pocket in advance, and then the same CP toolpath was used to machine the pocket. Its diagram of measured cutting forces is shown in Fig. 11b. It is observed that the abrupt cutting force fluctuation in the first run of machining (Fig. 11a) is completely avoided. It proves that the algorithm of critical regions identification

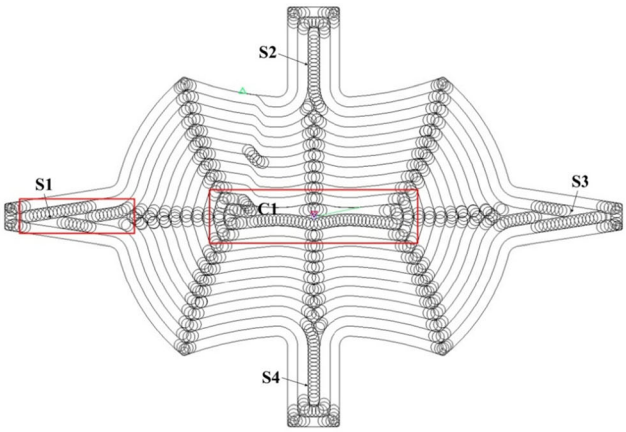

(a)

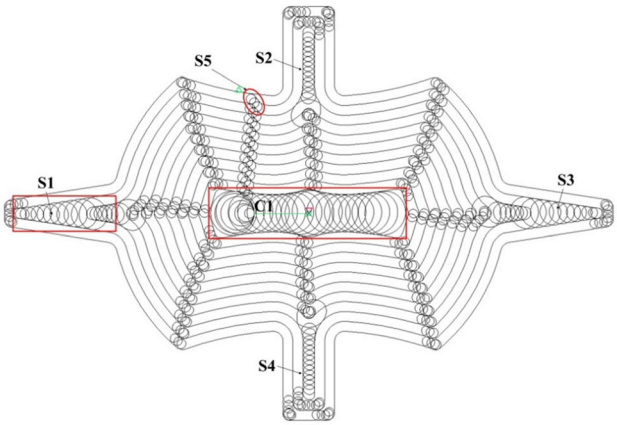

(b)

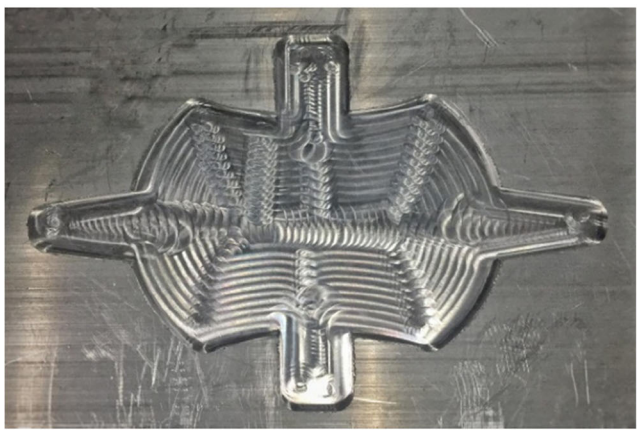

(c)

Fig. 12 A comparison of TR-CP-integrated milling strategies. **a** Toolpath by SIEMENS NX's TR solution. **b** Toolpath by RVTR-CP strategy. **c** The machined pocket by RVTR-CP toolpath

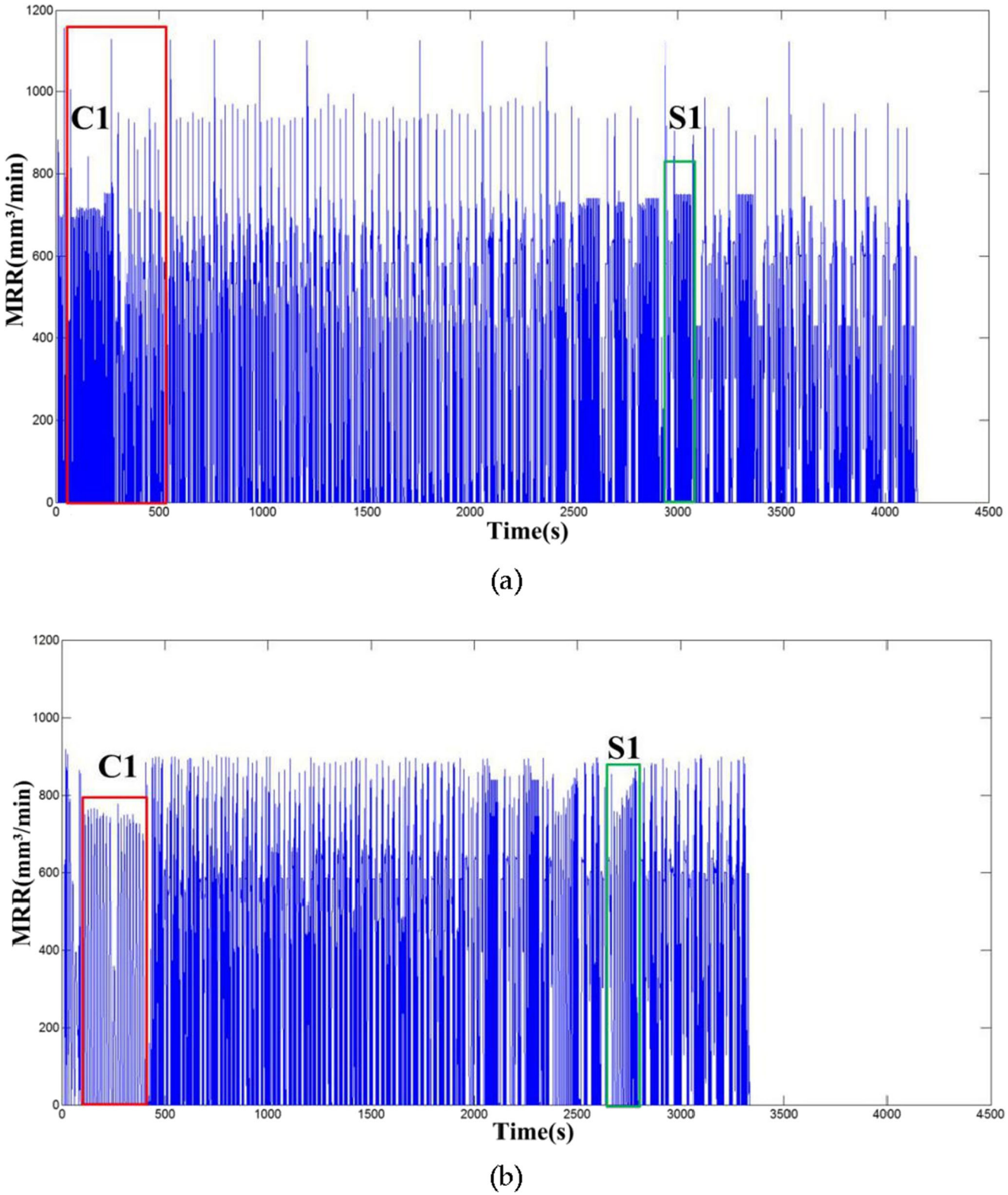

Fig. 13 MRR variation along TR-CP integrated toolpath. **a** The MRR variation with NX's toolpath. **b** The MRR variation with RVTR-CP toolpath

is accurate. Moreover, the maximal cutting force is greatly reduced by 28%, to about 180 N, and cutting force appears to be stabilized. This also indicated that the removal of critical regions from conventional CP machining is the right measure to minimize cutting force fluctuation.

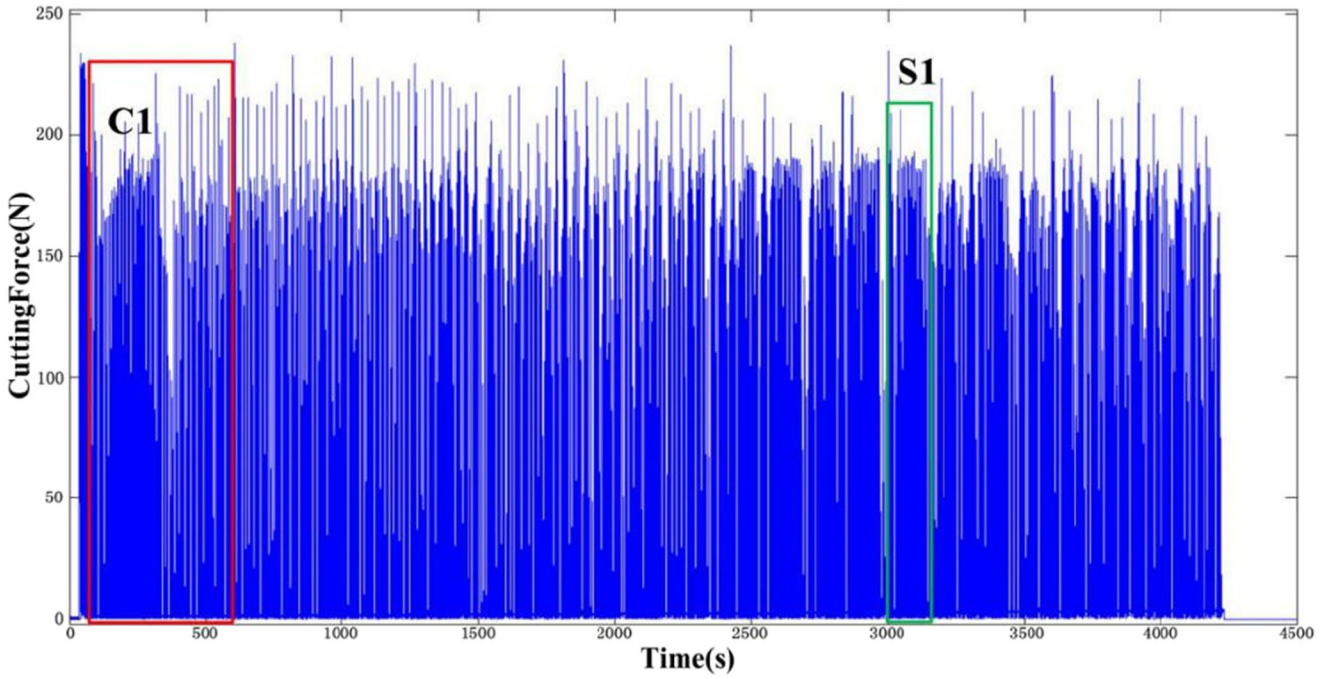

(a)

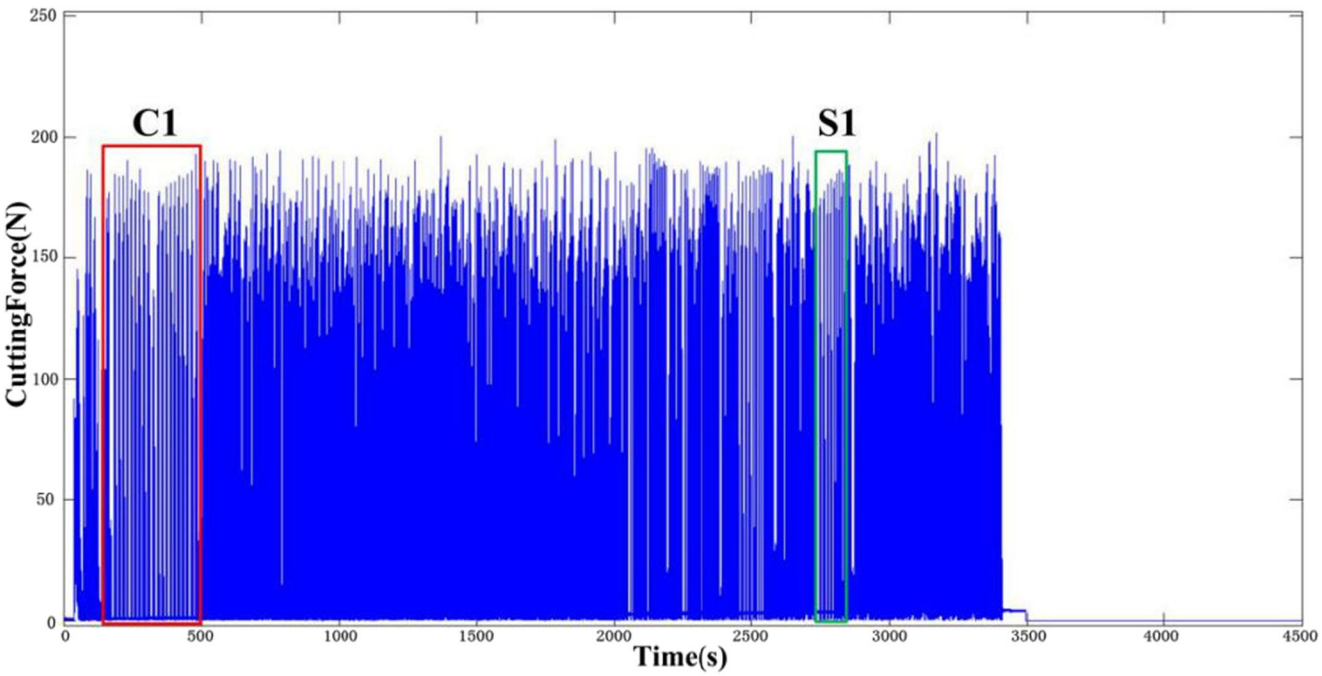

(b)

Fig. 14 Measured cutting forces for TR-CP integration toolpath. **a** The cutting forces with NX's toolpath. **b** The cutting forces with RVTR-CP toolpath

4.2 Performance evaluation of RVTR-CP toolpath

In this section, the performance evaluation for RVTR-CP toolpath is carried out from two aspects, i.e., the level of cutting force fluctuation and the efficiency of toolpath. For the purpose of comparative study, as shown in Fig. 12, the pocket was machined using the SIEMENS NX's TR toolpath and the proposed RVTR-CP toolpath, respectively.

Figure 12a shows the TR toolpath generated by SIEMENS NX, in which the toolpaths come with a constant TR radius

and a constant step for critical regions, and the rest of regions were still machined by conventional CP toolpath. From its MRR simulation (Fig. 13a) and actual cutting force measured (Fig. 14a), a number of cutting force shock can be observed during the machining, even though most of critical regions have been removed by TR milling before CP milling, these force shocks mostly happen when cutter moves across from one CP contour to the next. More than that, the simulation also shows that there could exist an obvious difference in MRR between TR milling and CP milling along the SIEMENS NX's toolpath. This problem is also demonstrated by the cutting force test shown in Fig. 14a, where the values of cutting force turn up and down drastically when the cutting is under transition between TR and CP toolpaths.

As a comparison, the above machining problem of cutting force fluctuation is well addressed with RVTR-CP toolpath. The most significant improvement is that the shocks of cutting forces are considerably minimized as shown by Fig. 14b. As discussed, such shocks happen mostly when the cutter moves across from one CP contour to the next, which is a typical issue with conventional CP milling. Owning to the critical region identification, the MRR variation when crossing CP contours is precisely captured, and a small portion of TR toolpath, as label by S*5* in Fig. 14b, is used to replace the direct linear connection between two parallel contours; this effectively prevents the cutting force shocks from happening.

Furthermore, with the contour fitting algorithm explained in Section 2.3, many small but neighboring critical regions now can be grouped into a connected critical region, for, e.g., the critical regions *S1, S3*, and *C1* in Fig. 12b. These grouped critical regions are more suitable for machining by a single stripe of RVTR toolpath. For the critical region milling only, the proposed RVTR toolpath has shown better performance than the TR milling toolpath by SIEMENS NX. Taking the TR milling of *C1* region for example, Fig. 13a shows that the MRR comes with obvious fluctuation when using the TR toolpath with constant radius by SIEMENS NX. This might be caused by the sharp changes of feed direction, for which multiple stripes of TR milling are required to fill up the irregular narrow region. Corresponding to such inconsistent MRR, the cutting force suffers several shocks when milling the region *C1*, as shown in Fig. 14a. As a comparison, the problem of cutting force shock when milling critical region is completely avoided by RVTR toolpath. As shown in Fig. 14b, since the irregular critical region can be removed by a single stripe of TR motion, there ends up with no force shocks happening.

Other than the advantage gained over cutting force control, the experimental results on the toolpath efficiency are reported in Table 1, where the RVTR-CP integration strategy also demonstrated considerable efficiency improvements over the TR-CP toolpath by SIEMENS NX. To be specific, the RVTR-CP strategy saved the total length of toolpath by 20.33%, comparing with that of SIEMENS NX toolpath. Meanwhile, better cutting conditions were achieved by the RVTR-CP strategy, since it decreased the maximum MRR by 21.81% and reduced the maximum cutting force by 15.92%, comparatively.

Table 1 Performance comparison between NX's TR-CP strategy and RVTR-CP strategy

Machining performances	NX's TR-CP strategy	RVTR-CP strategy	Improvements
Feedrate (mm/min)	100	100	–
Machining time (s)	4172	3323	20.35%
Length of toolpath (mm)	7040	5609	20.33%
Maximum MRR (mm^3/min)	1157	904.7	21.81%
Maximum force (N)	238.0	200.1	15.92%

5 Conclusions

This work presents a novel RVTR-CP toolpath integration strategy for high-performance machining of complex pockets. The main contributions of the proposed work include:

1. For the first time, the critical regions with complex pocket machining are identified based on quantitative analysis. This is carried out automatically by the intelligent evaluation of MRR change along the milling toolpath. With a given part pocket and its conventional CP toolpath, the proposed critical region identification algorithm can intelligently segment all the critical cutter locations from the rest of safe ones and then organize them into a number of critical regions with reasonable enclosing profiles for TR milling.
2. Based on the critical region recognition, the connection between RVTR trajectories with neighboring CP toolpaths is geometrically continuous and with very consistent MRR transition as well. This offers an almost constant cutting force for the entire pocket machining.

Experimental investigation shows that the proposed RVTR-CP integration can achieve much better performance comparing with the TR-CP milling function by current commercially available CAM software. In particular, it offers a favorable machining condition with minimized fluctuation of cutting forces and also with considerable decrease of the total length of toolpath; therefore, it is very suitable for high-performance machining of complex pockets.

Last but not the least, since the algorithms for critical region identification and the RVTR toolpath generation for regional milling are generic, the proposed approach can be further extended to address the cutting force fluctuation issues with other types of toolpaths, such as zigzag toolpath. Future

work is undergoing to develop specific methods of continuous geometric connection between RVTR trajectories with other types of toolpath.

Acknowledgements This work was supported by the National Nature Science Foundation of China [grant numbers 51575192 and 51775192] and the Science & Technology Research Program of Guangdong, China [grant numbers 2015B090922010 and 2017B010110010].

References

1. Choy HS, Chan KW (2003) Modeling cutter swept angle at cornering cut. Int J CAD/CAM 3(1):1–12
2. Ibaraki S, Yamaji I, Matsubara A (2010) On the removal of critical cutting regions by trochoidal grooving. Precis Eng 34(3):467–473. https://doi.org/10.1016/j.precisioneng.2010.01.007
3. Tarng YS, Cheng ST (1993) Fuzzy control of feed rate in end milling operations. Int J Mach Tools Manuf 33(4):643–650. https://doi.org/10.1016/0890-6955(93)90098-F
4. Erdim H, Lazoglu I, Ozturk B (2006) Feedrate scheduling strategies for free-form surfaces. Int J Mach Tools Manuf 46(7):747–757. https://doi.org/10.1016/j.ijmachtools.2005.07.036
5. Uddin MS, Ibaraki S, Matsubara A, Nishida S, Kakino Y (2007) A tool path modification approach to cutting engagement regulation for the improvement of machining accuracy in 2D milling with a straight end mill. J Manuf Sci Eng 129(6):1069–1079. https://doi.org/10.1115/1.2752526
6. Karunakaran KP, Shringi R, Ramamurthi D, Hariharan C (2010) Octree-based NC simulation system for optimization of feed rate in milling using instantaneous force model. Int J Adv Manuf Technol 46(5):465–490. https://doi.org/10.1007/s00170-009-2107-7
7. Choy HS, Chan KW (2003) A corner-looping based tool path for pocket milling. Comput Aided Des 35(2):155–166. https://doi.org/10.1016/S0010-4485(02)00049-0
8. Kim HC, Lee SG, Yang MY (2006) An optimized contour parallel tool path for 2D milling with flat end mill. Int J Adv Manuf Technol 31(5):567–573. https://doi.org/10.1007/s00170-005-0228-1
9. Held M, Spielberger C (2009) A smooth spiral tool path for high speed machining of 2D pockets. Comput Aided Des 41(7):539–550. https://doi.org/10.1016/j.cad.2009.04.002
10. Rauch M, Duc E, Hascoet JY (2009) Improving trochoidal tool paths generation and implementation using process constraints modeling. Int J Mach Tools Manuf 49(5):375–383. https://doi.org/10.1016/j.ijmachtools.2008.12.006
11. Elber G, Cohen E, Drake S (2005) MATHSM: medial axis transform toward high speed machining of pockets. Comput Aided Des 37(2):241–250. https://doi.org/10.1016/j.cad.2004.05.008
12. Ferreira JCE, Ochoa DM (2013) A method for generating trochoidal tool paths for 2D pocket milling process planning with multiple tools. Proc Inst Mech Eng Part B: J Eng Manuf 227(9):1287–1298. https://doi.org/10.1177/0954405413487897
13. Wu S, Ma W, Li B, Wang C (2016) Trochoidal machining for the high-speed milling of pockets. J Mater Process Technol 233:29–43. https://doi.org/10.1016/j.jmatprotec.2016.01.033
14. Wu S, Zhao Z, Wang CY, Xie Y, Ma W (2016) Optimization of toolpath with circular cycle transition for sharp corners in pocket milling. Int J Adv Manuf Technol 86(9–12):1–11. https://doi.org/10.1007/s00170-016-8364-3
15. Deng Q, Mo R, Chen ZC, Chang Z (2017) A new approach to generating trochoidal tool paths for effective corner machining. Int J Adv Manuf Technol 1–4:1–12. https://doi.org/10.1007/s00170-017-1353-3
16. Sun C, Wang YH, Huang ND (2015) A new plunge milling tool path generation method for radial depth control using medial axis transform. Int J Adv Manuf Technol 76(9–12):1575–1582. https://doi.org/10.1007/s00170-014-6375-5
17. Wang QH, Wang S, Jiang F, Li JR (2016) Adaptive trochoidal toolpath for complex pockets machining. Int J Prod Res 54(20):1–14. https://doi.org/10.1080/00207543.2016.1143135
18. Ohtsu N (1979) A threshold selection method from gray-level histograms. IEEE Transactions on Systems Man & Cybernetics 9(1):62–66. https://doi.org/10.1109/TSMC.1979.4310076
19. Edelsbrunner H, Kirkpatrick DG, Seidel R (1983) On the shape of a set of points in the plane. IEEE Trans Inf Theory 29(4):551–559. https://doi.org/10.1109/TIT.1983.1056714
20. Otkur M, Lazoglu I (2007) Trochoidal milling. Int J Mach Tools Manuf 47(9):1324–1332. https://doi.org/10.1016/j.ijmachtools.2006.08.002
21. Held M (2001) VRONI: an engineering approach to the reliable and efficient computation of voronoi diagrams of points and line segments. Comput Geom 18(2):95–123. https://doi.org/10.1016/S0925-7721(01)00003-7
22. Kloypayan J, Lee YS (2002) Material engagement analysis of different endmills for adaptive feedrate control in milling processes. Comput Ind 47(1):55–76. https://doi.org/10.1016/S0166-3615(01)00136-1